Journal of Information Systems Engineering and Management
2025, 10(43s)

e-ISSN: 2468-4376

https://www.jisem-journal.com/

Research Article

A Compact Circular Patch Antenna with Adaptive Beam Steering and Band Notch Filtering for UWB Applications

Hanumanthappa Magalada [1], Dr. Chandrappa D N [2], Dr. Yogesh G S [3]

[1] *Assistant Professor & Research Scholar, Department of Electronics & Communication Engineering, PES Institute of Technology and Management, Shivamogga, Affiliated to Visvesvaraya Technological University Belagavi - 590018, Karnataka, India. Email: magalada@pestrust.edu.in*

[2] *Associate Professor, Department of Electronics & Communication Engineering, East Point College of Engineering & Technology, Bangalore, Affiliated to Visvesvaraya Technological University Belagavi - 590018, Karnataka, India. Email: chandrappa@eastpoint.ac.in*

[3] *Professor & Head, Department of Electronics & Communication Engineering, East Point College of Engineering & Technology, Bangalore, Affiliated to Visvesvaraya Technological University Belagavi - 590018, Karnataka, India. Email: gs.yogesh@eastpoint.ac.in*

ARTICLE INFO

Received: 22 Dec 2024

Revised: 18 Feb 2025

Accepted: 26 Feb 2025

ABSTRACT

This paper presents a compact circular patch antenna specifically designed for ultra-wideband (UWB) applications, operating efficiently across the 2–6 GHz frequency range. A dedicated notch at 2.4 GHz is incorporated to effectively suppress interference from WLAN signals. The antenna is fabricated on an FR4 substrate with compact dimensions of 35 × 32 × 1 mm³, offering a low-profile solution ideal for integration into modern wireless systems. To enhance functionality, three precisely engineered rectangular slots are introduced—two on the ground plane to influence the radiation pattern and one on the patch to achieve the desired notch behavior. Beam steering capability is enabled via diodes D3 and D4, allowing directional reconfiguration up to ±60°, with observed gain variations between 3.8 dB and 4.5 dB. Simulated and measured results exhibit strong agreement, with only minor deviations—0.1 GHz in notch frequency and 0.1 dB in gain—validating the design's precision. Compared to traditional UWB monopole and patch antennas, the proposed antenna offers a smaller footprint, efficient interference rejection, and enhanced beam steering, making it a promising candidate for next-generation adaptive wireless communication systems.

Keywords: Beam Steering, Interference Suppression, Reconfigurable Antenna, Ultra-Wideband (UWB).

INTRODUCTION

As digital communication technologies continue to advance, innovations in wireless systems are accelerating rapidly [1]. Central to these developments are antennas, which directly influence the performance of wireless networks. The rapid growth of smart devices and expanding communication infrastructures has created a growing demand for antennas that are not only compact but also highly flexible and adaptable [2]. Traditional antenna designs, while effective for many applications, lack the versatility needed to keep pace with evolving communication requirements [3]. Their fixed operational characteristics limit their ability to support dynamic environments that require multi-band functionality, adaptability to varying signal conditions, and performance in diverse propagation scenarios [4–5].

To overcome these limitations, researchers have increasingly focused on reconfigurable antennas. These advanced antennas are capable of altering key operational parameters—such as frequency, polarization, and radiation pattern—in real time, allowing them to adapt to changing environmental and system demands. This dynamic behavior leads to enhanced performance, reliability, and efficiency across a wide range of wireless applications [6–10]. The rising interest in reconfigurable antennas has driven significant progress in both their conceptual design and practical implementation.

Journal of Information Systems Engineering and Management
2025, 10(43s)
e-ISSN: 2468-4376
https://www.jisem-journal.com/

Research Article

Among various reconfiguration techniques, electrical switching is one of the most commonly used approaches due to its ability to provide real-time control over antenna parameters. Components such as PIN diodes, varactor diodes, micro-electro-mechanical systems (MEMS), and optical switches are often integrated into antenna structures to facilitate these adjustments [11–15]. These components work by changing the current path within the antenna, thereby modifying surface currents and enabling different operational modes. Because of their ease of integration and relatively simple control mechanisms, electrical switches have been extensively researched. For instance, in 2022, Palsokar and Lahudkar proposed a rectangular patch antenna that used a single PIN diode to switch between three operating frequencies—2.47 GHz, 3.8 GHz, and 5.36 GHz—while maintaining a simplified biasing network [16–17].

Varactor diodes offer another effective reconfiguration method by allowing continuous tuning of frequency through variable capacitance controlled by a bias voltage.

Row and Chen (2022) demonstrated this with a patch antenna that incorporated two varactors placed between the radiating patch and the ground plane. This design achieved a tuning range from 3.3 GHz to 4.2 GHz, showing a broader frequency adjustability compared to PIN-diode-based approaches [18–19]. MEMS switches represent a more mechanically integrated solution, combining sensors, actuators, and other components fabricated using semiconductor processes. These switches provide benefits like low insertion loss and high reliability. A notable example is the work by Kingsley et al. (2007), who designed a CPW-fed monopole antenna using a three-stage Sierpinski fractal structure with MEMS switches to enable frequency reconfiguration. Their system required no external biasing circuit and produced stable radiation characteristics. However, a notable drawback of MEMS is their relatively slow switching speeds, typically ranging from 1 to 200 seconds, which may be unsuitable for certain fast-response applications [20–23]. Another form of reconfiguration involves optical switches, which utilize semiconductor materials and optical biasing rather than traditional metallic components. These are mainly used in niche systems, such as infrared-based communication, due to their bulkier design and complex integration requirements.

Beyond electrical methods, structural reconfiguration offers alternative ways to achieve antenna adaptability. Approaches like origami-inspired folding, microfluidic manipulation, and mechanical transformations allow the antenna's geometry to be physically modified, eliminating the need for complex control circuitry. Such methods are particularly attractive for their high power handling and low signal loss. For example, Yao et al. developed an origami-style Nojima antenna capable of tuning both frequency and radiation pattern. When folded, it resonated at 1.61 GHz with a directional beam, and when unfolded, it shifted to 0.66 GHz with an omnidirectional pattern [24].

Microfluidic and mechanical systems are also being employed to enable reconfigurable designs. In 2009, So et al. introduced an antenna that adjusted its dipole length by injecting a eutectic gallium-indium (EGaIn) alloy. Later, in 2017, Yang et al. used micromotors placed underneath antenna elements to rotate resonators for frequency tuning.

Recent breakthroughs in materials science have opened new possibilities for reconfigurable antennas. Innovative materials like liquid dielectrics, graphene, and shape memory alloys offer electrical tunability in response to environmental stimuli. In 2020, Ren et al. designed a radiation pattern and polarization reconfigurable antenna using a central dielectric resonator flanked by tunable parasitic dielectric elements controlled by fluid flow. Graphene, known for its exceptional tunability and conductivity, has become a popular choice for terahertz antennas. In 2012, Huang et al. proposed a graphene-based beam-steerable terahertz antenna, which achieved beam steering within a ±30° range by adjusting applied voltages.

Shape memory alloys (SMAs) are also gaining traction due to their ability to change shape with heat. Sumana and Florence (2020) introduced an antenna using SMA rectangular patches; by selectively heating them, they could steer the beam to 330° or 30°, enabling effective pattern reconfiguration [25].

A newer approach involves the use of bistable composite materials, which can hold two stable states without continuous energy input. These composites combine structural reconfigurability with material responsiveness. In 2023, Huang et al. presented a bistable reconfigurable antenna that responded to light-based stimuli. The antenna's

Journal of Information Systems Engineering and Management
2025, 10(43s)
e-ISSN: 2468-4376
https://www.jisem-journal.com/

Research Article

radiation properties could be altered by transitioning between its two stable states, triggered by a snapping mechanism, showcasing a unique combination of passive and responsive reconfiguration capabilities.

ANTENNA DESIGN

This section outlines the design of the proposed antenna, as shown in Figure 1, which features a circular patch with a partially truncated ground plane and carefully etched edges to enhance overall performance. The antenna utilizes a microstrip line feeding mechanism, ensuring efficient power transfer and proper impedance matching. It is built on an FR4 epoxy substrate, a widely used dielectric material valued for its affordability, mechanical stability, and reliable electrical properties. A distinctive aspect of this design is the inclusion of two symmetrical extensions on either side of the circular patch. These extensions play a crucial role in enabling dual band operation by modifying the surface current distribution and influencing the resonance characteristics. The partial truncation of the ground plane further contributes to impedance matching across the intended frequency bands, leading to improved bandwidth and radiation efficiency. Additionally, the etched edges of the ground plane help optimize current flow, reducing unwanted signal reflections and enhancing overall antenna performance. To further improve functionality, three rectangular slots are strategically incorporated into the structure. Two of these slots are embedded in the ground plane to modify the radiation characteristics, facilitating pattern tilting. The third slot, positioned on the patch, generates a band notch effect, effectively suppressing interference from unwanted frequency bands. The antenna achieves reconfigurability through the integration of multiple PIN diodes. Specifically, diodes D1 and D2 are placed on the extensions to enable frequency reconfiguration, while diode D4 is positioned within the patch slot to dynamically control the notch function. Additionally, diodes D3 and D4, embedded within the ground plane slots, enable adaptive pattern reconfiguration. This dynamic tuning capability enhances the versatility of the antenna, making it well suited for applications that require flexible frequency selection and radiation pattern control.

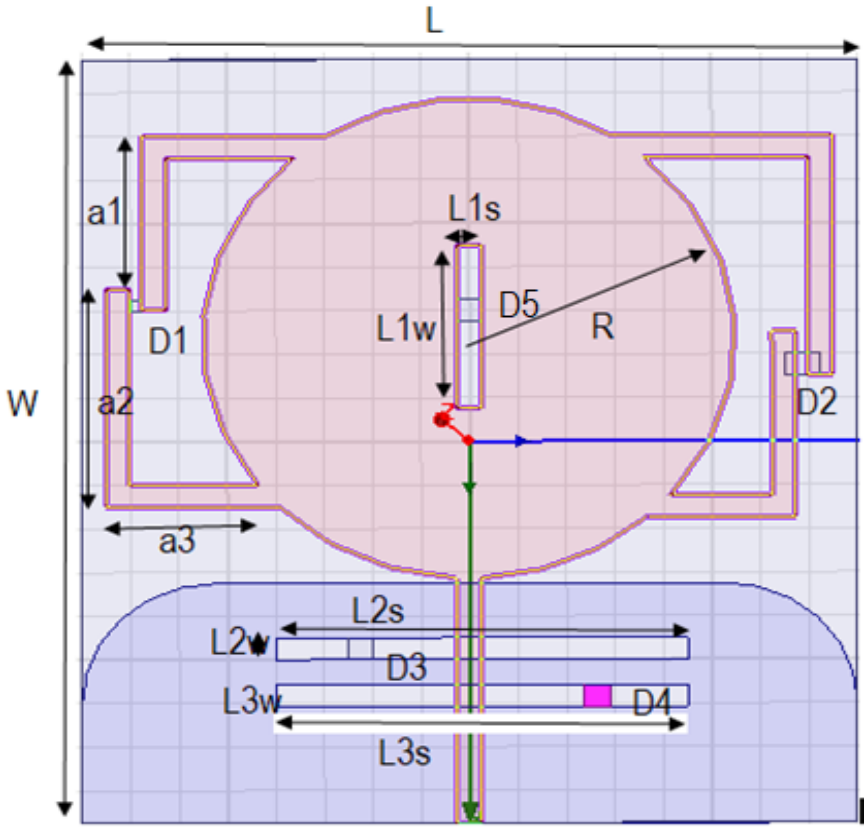

Figure 1. Proposed Antenna Design

Journal of Information Systems Engineering and Management
2025, 10(43s)
e-ISSN: 2468-4376
https://www.jisem-journal.com/

Research Article

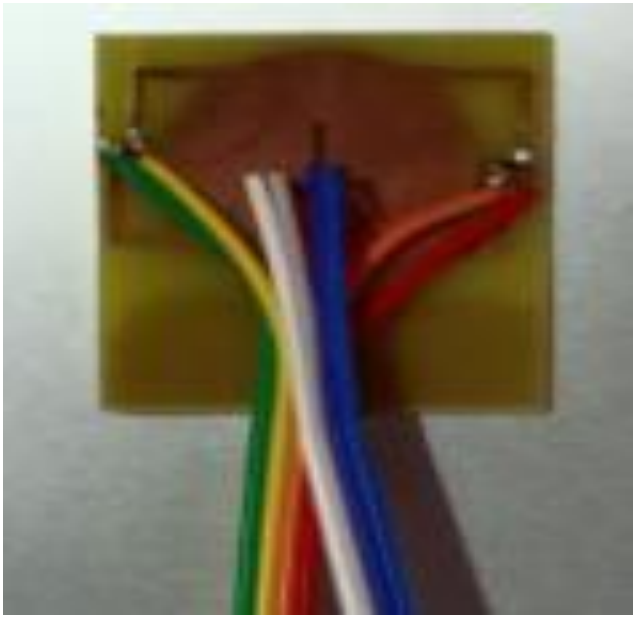

Figure 2. Fabricated Prototypes

Table 1. Antenna Specifications

Parameter	Value in mm
L	35mm
W	32mm
A1	8mm
A2	10mm
A3	7.1mm
R	11mm
L1s	1mm
L1w	7.5mm
L2s	17mm
L2w	1mm
L3s	17mm
L3w	1mm

RESULTS AND DISCUSSION

Figures 3 to 5 illustrate the antenna's performance under different switching states of diodes D1 and D2, providing valuable insights into changes in operating frequency, return loss, voltage standing wave ratio, gain, and radiation characteristics based on their ON and OFF positions. When diode D1 is switched ON, as shown in Figure 3, the antenna operates at 2.4 gigahertz, achieving a return loss of negative 42 decibels, a voltage standing wave ratio below 2 (Figure 4), and a gain of 1.4 decibels (Figure 5). Turning D1 OFF shifts the resonance frequency to 3.9 gigahertz, with a return loss of negative 39 decibels, while the voltage standing wave ratio remains below 2, and the gain slightly

Journal of Information Systems Engineering and Management
2025, 10(43s)
e-ISSN: 2468-4376
https://www.jisem-journal.com/

Research Article

decreases to 1.3 decibels. Similarly, activating diode D2 results in an operating frequency of 5.5 gigahertz, with a return loss of negative 45 decibels, a voltage standing wave ratio under 2, and a gain of 1.2 decibels. When D2 is turned OFF, the frequency moves to 6.8 gigahertz, maintaining a return loss of negative 44 decibels, a voltage standing wave ratio below 2, and a slight decrease in gain to 1.1 decibels. Despite these shifts in frequency, the radiation angle remains fixed at 0 degrees, indicating that the antenna's radiation pattern remains unchanged across different configurations. The consistently low return loss across all cases confirms effective impedance matching with minimal signal reflection. Additionally, the voltage standing wave ratio staying below 2 in all conditions highlights stable antenna performance across different switching states. Table 2 provides a summary of these results, demonstrating the antenna's capability to achieve frequency reconfiguration through diode control. This adaptability makes it a strong candidate for multi band applications that require dynamic tuning of operational frequencies.

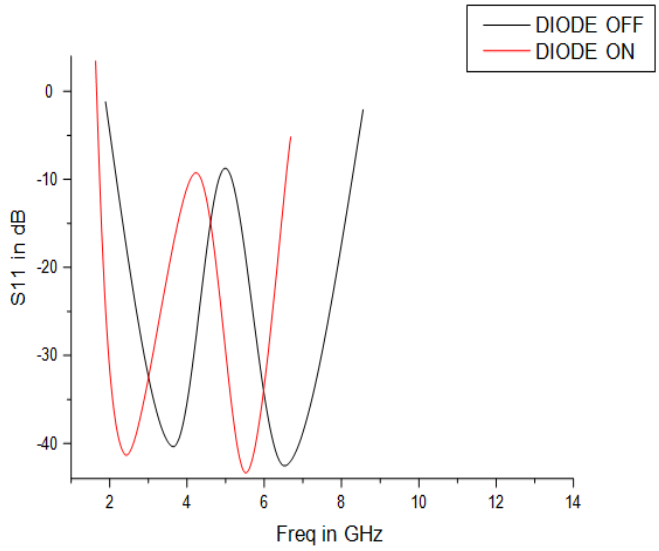

Figure 3. Return Loss Plot when D1 and D2 is ON

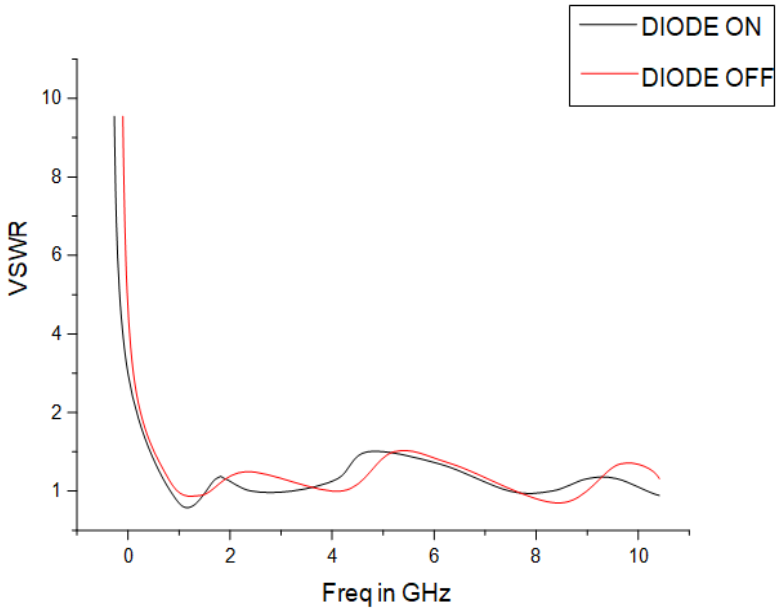

Figure 4. VSWR Plot for D1 and D2 diode conditions

Journal of Information Systems Engineering and Management
2025, 10(43s)
e-ISSN: 2468-4376
https://www.jisem-journal.com/

Research Article

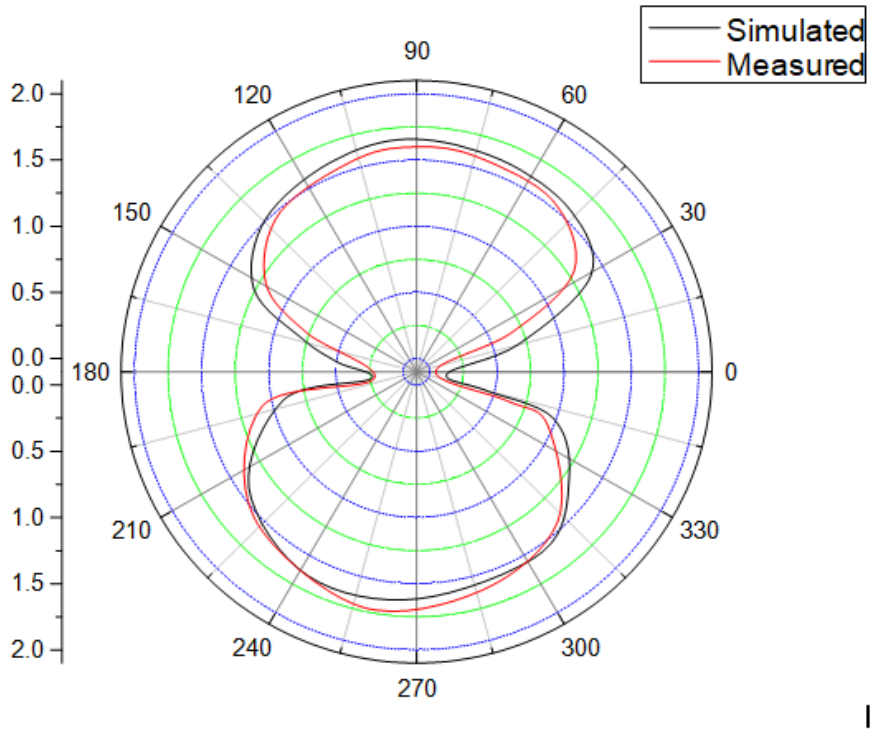

Figure 5 Radiation Plot of the Proposed Antenna

Table 2 Summary of Results for Diodes D1 and D2 conditions

Parameters	D1		D2	
	ON	OFF	ON	OFF
Freq in GHz	2.4	3.9	5.5	6.8
Return Loss in dB	-42	-39	-45	-44
VSWR	<2	<2	<2	<2
Gain in dB	1.4	1.3	1.2	1.1
Angle in deg	0	0	0	0

Figure 6 illustrates the impact of the switching state of diode D5 on the antenna's band-notch frequency, return loss, VSWR, gain, and radiation angle. When D5 is in the ON state, the band-notch frequency is set at 2.4 GHz, with a return loss of -3.5 dB. The voltage standing wave ratio (VSWR) in this state is relatively high at 5.4, indicating impedance mismatch. The antenna gain is 0.9 dB (Figure 8), and the radiation angle remains at 0 degrees.

When D5 is turned OFF the band notch frequency shifts to 3.5 GHz with an improved return loss of -2 dB. The VSWR significantly decreases to 1.2, suggesting better impedance matching and reduced signal reflection. The antenna gain also increases considerably to 3.9 dB, while the radiation angle remains unchanged at 0 degrees. These results highlight the role of diode D5 in dynamically controlling the band-notch functionality. The ON state results in a higher VSWR and lower gain, which may be used to suppress interference at a specific frequency. Meanwhile, the OFF state provides better impedance matching and higher gain, making the antenna more efficient at its operational frequency. This demonstrates the antenna's ability to achieve reconfigurable band-notching, making it adaptable for various wireless communication applications where interference mitigation is necessary. The summary is presented in Table 3

Journal of Information Systems Engineering and Management
2025, 10(43s)
e-ISSN: 2468-4376
https://www.jisem-journal.com/

Research Article

Table 3 Summary of Results for D5

Parameter	D5 ON	D5 OFF
Band Notch Freq in GHz	2.4	3.5
Return Loss in dB	-3.5	-2
VSWR	5.4	1.2
Gain in dB	0.9	3.9
Angle in deg	0	0

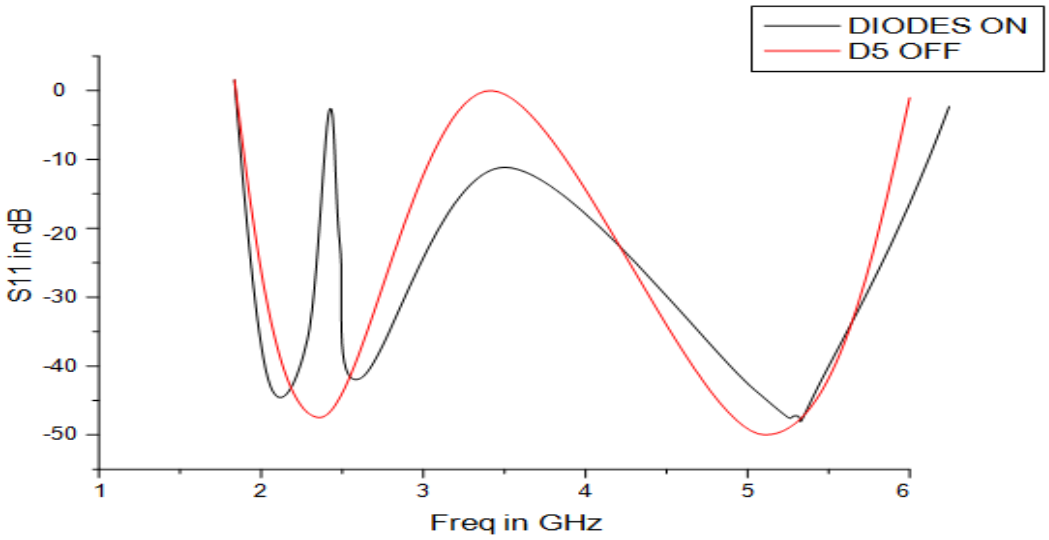

Figure 6 Return Loss Plot of the Proposed Antenna when D5 is ON

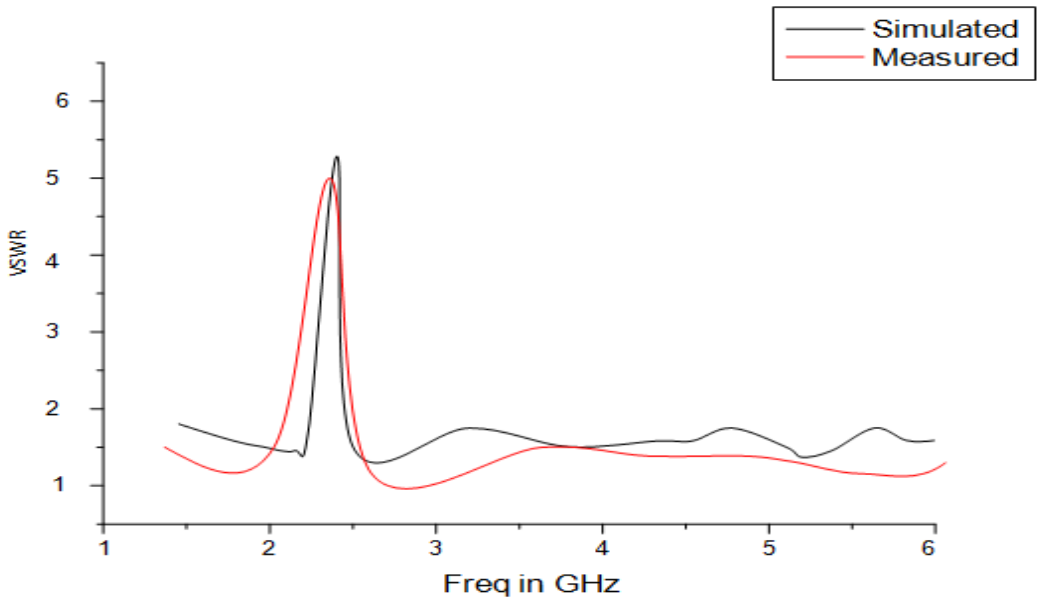

Figure 7 VSWR Plot of the antenna when D5 in ON

Journal of Information Systems Engineering and Management
2025, 10(43s)
e-ISSN: 2468-4376
https://www.jisem-journal.com/

Research Article

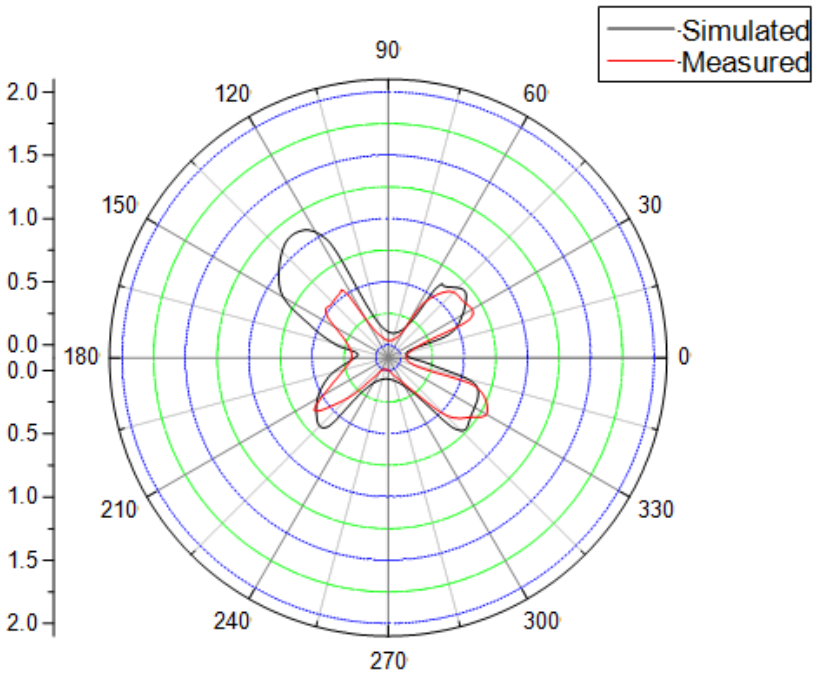

Figure 8 Radiation Pattern when D5 in ON

Figure 9 presents a comparison between simulated and measured results for key antenna parameters, including band-notch frequency, voltage standing wave ratio (VSWR), and gain. The simulated band-notch frequency is observed at 2.4 GHz, whereas the measured value is slightly shifted to 2.5 GHz, indicating a minor deviation likely due to fabrication tolerances or environmental factors affecting the testing conditions.

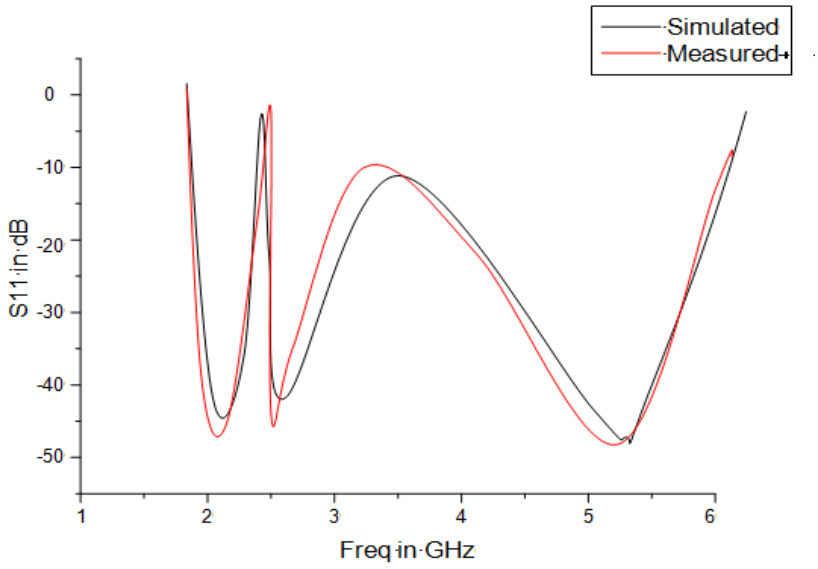

Figure 9 Simulated and Measured Results for D5 ON condition

Figure 10 & Figure 11 presents the effect of switching states of diodes D3 and D4 on the antenna's gain and beam direction. When D3 is in the ON state, the antenna achieves a gain of 3.9 dB with a beam tilt of -60 degrees, whereas when D3 is turned OFF, the gain reduces to 3 dB, and the beam direction returns to 0 degrees. Similarly, when D4 is

Journal of Information Systems Engineering and Management
2025, 10(43s)
e-ISSN: 2468-4376
https://www.jisem-journal.com/

Research Article

switched ON, the gain increases to 4.5 dB, and the beam shifts to 60 degrees. However, when D4 is OFF, the gain drops to 3 dB, and the radiation angle reverts to 0 degrees.

These results highlight the role of diodes D3 and D4 in dynamically controlling both gain and radiation direction. The ON states of these diodes enable beam steering, with D3 directing the beam towards -60 degrees and D4 shifts it to 60 degrees. Meanwhile, in their OFF states, the antenna maintains a neutral beam direction. This functionality enhances the adaptability of the antenna, making it suitable for applications requiring pattern reconfigurability, such as beamforming in wireless communication systems. The ability to adjust gain and beam angle dynamically provides improved signal coverage and better system performance.

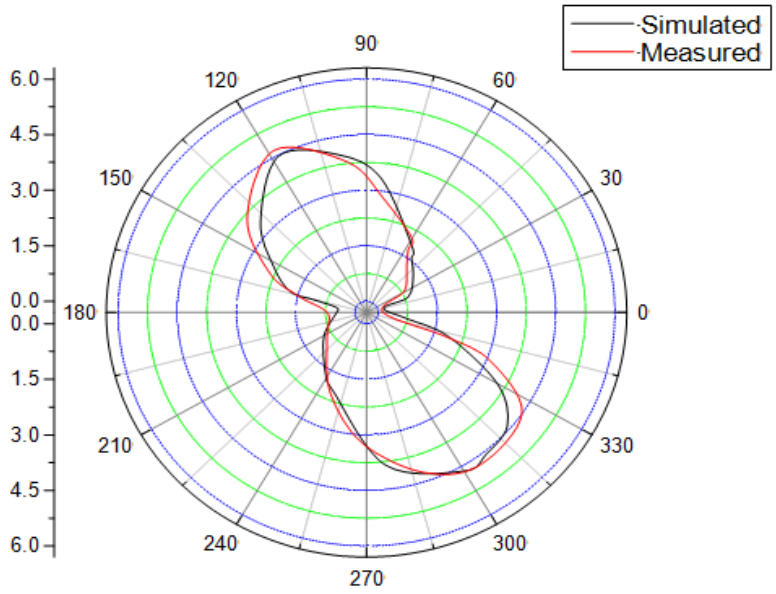

Figure 10 Radiation Pattern of the antenna when D3 is ON

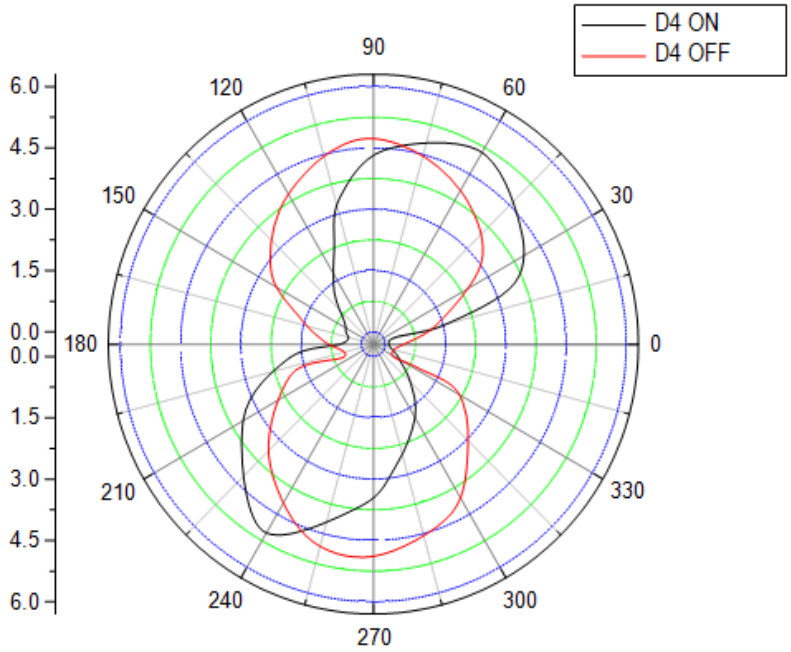

Figure 11 Radiation Pattern of the antenna when D4 is ON

Journal of Information Systems Engineering and Management
2025, 10(43s)
e-ISSN: 2468-4376
https://www.jisem-journal.com/

Research Article

The Table 4 provides a comparison between the simulated and measured values of gain and beam angle for the antenna when D3 is ON. The simulated gain is 3.9 dB, while the measured gain is slightly lower at 3.8 dB, indicating a minor deviation likely due to fabrication tolerances or environmental factors during testing. Despite this small difference, the measured gain closely aligns with the simulated value, validating the accuracy of the design. The beam angle remains consistent at -60 degrees in both simulations and practical measurements, demonstrating that the antenna maintains its intended directional radiation characteristics. The close agreement between the simulated and measured results confirms the reliability and effectiveness of the antenna design, ensuring its suitability for real-world applications.

Table 4 Summaries of Simulated and Measured Results for D3 ON

Parameters	Simulated	Measured
Gain	3.9	3.8
Angle in dB	-60	-60

The Table 5 compares the simulated and measured values of gain and beam angle for the antenna. The simulated gain is 4.5 dB, while the measured gain is slightly lower at 4 dB, which may be attributed to fabrication imperfections, material losses, or environmental factors during testing. Despite this minor variation, the measured gain closely aligns with the simulated result, confirming the accuracy and reliability of the design. The beam angle remains unchanged at 60 degrees in both simulated and measured results, demonstrating the antenna's consistent directional radiation performance. The close agreement between these values indicates that the antenna functions as expected in real-world conditions, making it a suitable candidate for applications requiring directional beam control and reliable performance.

Table 5 Summaries of Simulated and Measured Results for D4 ON

Parameters	Simulated	Measured
Gain	4.5	4
Angle in dB	60	60

Table 6 Comparison with Previous Works

Reference	Antenna Type	Substrate	Size (mm^3)	Frequency Range (GHz)
[26]	UWB Monopole	FR4	30 × 25 × 1.6	3.1–10.6 (Notches: 3.5, 5.5
[27]	UWB Patch	Rogers RO4350	28 × 20 × 0.8	3.0–11.0 (Notches: 3.5, 5.8)
[28]	UWB Monopole	FR4	35 × 30 × 1.6	2.8–12.0 (Notches: 2.4, 5.2)
[29]	Monopole with SRR	Rogers RT5880	25 × 25 × 0.8	3.2–10.8 (Notches: 3.3, 5.5)
[30]	UWB Circular Monopole	FR4	32 × 28 × 1.6	3.0–11.5 (Notches: 3.4, 5.6)
Proposed Antenna	**Circular Patch**	**Fr4**	**35 x32 x 1**	**2 – 6 (Notch – 2.4 GHz)**

The table provides a comparative analysis of different ultra wide band (UWB) antennas from various research works, focusing on antenna type, substrate material, size, and operating frequency range, including notch bands. The antennas reviewed include monopole, patch, and circular monopole designs, utilizing substrates such as FR4, Rogers RO4350, and Rogers RT5880. The frequency ranges for these antennas typically span from approximately 2.8 GHz to 12 GHz, with notch bands implemented at different frequencies to mitigate interference from undesired signals.

Journal of Information Systems Engineering and Management
2025, 10(43s)
e-ISSN: 2468-4376
https://www.jisem-journal.com/

Research Article

The proposed circular patch antenna, designed using an FR4 substrate with dimensions of 35 × 32 × 1 mm³, operates within a frequency range of 2–6 GHz with a single notch at 2.4 GHz. Compared to previous designs, the proposed antenna offers a more compact form factor while maintaining effective UWB operation. Unlike designs that employ multiple notch bands, this antenna specifically targets interference at 2.4 GHz, which is beneficial for mitigating WLAN interference while maintaining performance in other bands. Furthermore, the use of a circular patch configuration enhances radiation characteristics, providing better stability and polarization control compared to traditional monopole structures.

A key advantage of the proposed design is its compact size compared to other UWB monopole antennas, such as those by Sharma et al. (2022) and Kumar et al. (2020), which use FR4 substrates but have larger dimensions. Additionally, while some existing works rely on high-performance substrates like Rogers RO4350 and RT5880 for improved efficiency, the proposed antenna demonstrates that a cost-effective FR4 substrate can still achieve desirable performance, making it more practical for real-world applications. This balance of size, material efficiency, and selective notch filtering makes the proposed antenna a strong candidate for modern wireless communication systems requiring interference suppression and stable UWB operation.

CONCLUSION

This paper explores the design and analysis of a compact circular patch antenna that operates within the 2 to 6 gigahertz frequency range, incorporating a single notch at 2.4 gigahertz to reduce interference. Compared to traditional ultra wideband antennas, the proposed design offers an optimal balance of compact size (35 by 32 by 1 cubic millimeters), cost effectiveness with an FR4 substrate, and reliable interference suppression. The measured performance closely aligns with simulated results, with only minor differences of 0.1 decibels in gain and 0.1 gigahertz in notch frequency, confirming the accuracy and reliability of the design. Additionally, the antenna features pattern reconfiguration through the use of diodes, allowing beam steering at plus or minus 60 degrees with a gain variation between 3.8 and 4.5 decibels. This enhances its adaptability for dynamic communication environments. Overall, this antenna offers a practical solution for ultra wideband applications, providing interference reduction, directional flexibility, and a compact structure, making it a strong choice for modern wireless communication systems.

REFERENCES

[1] S. M. Salleh, M. Jusoh, A. H. Ismail, et al., “Textile Antenna With Simultaneous Frequency and Polarization Reconfiguration for WBAN,” IEEE Access, vol. 6, no. 1, pp. 7350–7358, 2018, doi: 10.1109/ACCESS.2017.2787018.

[2] H. A. Majid, M. K. Rahim, M. R. Hamid, et al., “Frequency and Pattern Reconfigurable Slot Antenna,” IEEE Transactions on Antennas and Propagation, vol. 62, no. 10, pp. 5339–5343, 2014, doi: 10.1109/TAP.2014.2342237.

[3] S. Dubal and A. Chaudhari, “Mechanisms of Reconfigurable Antenna: A Review,” in Proc. 10th Int. Conf. Cloud Computing, Data Science & Engineering (Confluence), 2020, doi: 10.1109/Confluence47617.2020.9057998.

[4] N. O. Parchin, H. J. Basherlou, Y. I. Al-Yasir, et al., “Recent Developments of Reconfigurable Antennas for Current and Future Wireless Communication Systems,” Electronics, vol. 8, no. 2, 2019, doi: 10.3390/electronics8020128.

[5] M. Hussain, W. A. Awan, M. S. Alzaidi, et al., “Metamaterials and Their Application in the Performance Enhancement of Reconfigurable Antennas: A Review,” Micromachines, vol. 14, no. 2, pp. 349–375, 2023, doi: 10.3390/mi14020349.

[6] C. Liu, F. Yang, S. Xu, et al., “An E-Band Reconfigurable Reflectarray Antenna Using P-I-N Diodes for Millimeter-Wave Communications,” IEEE Transactions on Antennas and Propagation, vol. 71, no. 8, pp. 6924–6929, 2023, doi: 10.1109/TAP.2023.3291087.

[7] Q. Chen, J. Ala-Laurinaho, A. Khripkov, et al., “Varactor-Based Frequency-Reconfigurable Dual-Polarized Mm-Wave Antenna Array for Mobile Devices,” IEEE Transactions on Antennas and Propagation, vol. 71, no. 8, pp. 6628–6638, 2023, doi: 10.1109/TAP.2023.3287679.

[8] J. Navarajan, M. R. E. Jebarani, et al., "Design of Frequency Reconfigurable Antenna Based on Mc-Mems Switch," AEU Int. J. Electron. Commun., vol. 171, pp. 154911–154924, 2023, doi: 10.1016/j.aeue.2023.154911.
[9] V. Reji and C. T. Manimegalai, "Light Controlled Frequency Reconfigurable Antenna for Wireless Applications," Int. J. Microw. Wireless Technol., vol. 15, no. 1, pp. 143–149, 2023, doi: 10.1017/S1759078722000137.
[10] A. A. Palsokar and S. L. Lahudkar, "Frequency and Pattern Reconfigurable Rectangular Patch Antenna Using Single PIN Diode," AEU Int. J. Electron. Commun., vol. 10, no. 125, 2020, doi: 10.1016/j.aeue.2020.153370.
[11] J. S. Row and J. Y. Chen, "A Novel Design for Frequency Reconfigurable Antennas," Microw. Opt. Technol. Lett., vol. 64, no. 10, pp. 1815–1820, 2022, doi: 10.1002/mop.33371.
[12] G. M. Rebeiz, *RF MEMS: Theory, Design, and Technology*, Hoboken, NJ: John Wiley & Sons, 2004, doi: 10.1002/0471225282.
[13] Y. Shi and Z. Shen, "Recent Advances in Flexible RF MEMS," Micromachines, vol. 13, no. 7, 2022, doi: 10.3390/mi13071088.
[14] N. Kingsley, D. E. Anagnostou, M. Tentzeris, et al., "RF MEMS Sequentially Reconfigurable Sierpinski Antenna on a Flexible Organic Substrate With Novel DC-Biasing Technique," J. Microelectromech. Syst., vol. 16, no. 5, pp. 1185–1192, 2007, doi: 10.1109/JMEMS.2007.902462.
[15] C. G. Christodoulou, Y. Tawk, S. A. Lane, et al., "Reconfigurable Antennas for Wireless and Space Applications," Proc. IEEE, vol. 100, no. 7, pp. 2250–2261, 2012, doi: 10.1109/JPROC.2012.2188249.
[16] N. O. Parchin, H. J. Basherlou, Y. I. A. Al-Yasir, et al., "Reconfigurable Antennas: Switching Techniques—A Survey," Electronics, vol. 9, no. 2, pp. 336–350, 2020, doi: 10.3390/electronics9020336.
[17] C. Panagamuwa, A. Chauraya, J. Vardaxoglou, et al., "Frequency and Beam Reconfigurable Antenna Using Photoconducting Switches," IEEE Transactions on Antennas and Propagation, vol. 54, no. 2, pp. 449–454, 2006, doi: 10.1109/TAP.2005.863393.
[18] A. Petosa, "An Overview of Tuning Techniques for Frequency-Agile Antennas," IEEE Antennas Propag. Mag., vol. 54, no. 5, pp. 271–296, 2012, doi: 10.1109/MAP.2012.6348178.
[19] S. I. H. Shah and S. Lim, "Review on Recent Origami Inspired Antennas From Microwave to Terahertz Regime," Mater. Des., vol. 198, no. 1, pp. 109345–109360, 2021, doi: 10.1016/j.matdes.2020.109345.
[20] S. Yao, X. Liu, and S. V. Georgakopoulos, "A Mode Reconfigurable Nojima Origami Antenna," in IEEE Int. Symp. Antennas Propag. USNC/URSI Nat. Radio Sci. Meeting, 2015, doi: 10.1109/APS.2015.7305507.
[21] J. H. So, J. Thelen, A. Qusba, et al., "Reversibly Deformable and Mechanically Tunable Fluidic Antennas," Adv. Funct. Mater., vol. 19, no. 22, pp. 3632–3637, 2009, doi: 10.1002/adfm.200900604.
[22] X. Yang, S. Xu, F. Yang, et al., "A Broadband High-Efficiency Reconfigurable Reflectarray Antenna Using Mechanically Rotational Elements," IEEE Transactions on Antennas and Propagation, vol. 65, no. 8, pp. 3959–3966, 2017, doi: 10.1109/TAP.2017.2708079.
[23] Z. Chen and H. Wong, "Liquid Dielectric Resonator Antenna With Circular Polarization Reconfigurability," IEEE Transactions on Antennas and Propagation, vol. 66, no. 1, pp. 444–449, 2018, doi: 10.1109/TAP.2017.2762005.
[24] K. Moradi, A. Pourziad, and S. Nikmehr, "A Frequency Reconfigurable Microstrip Antenna Based on Graphene in Terahertz Regime," Optik, vol. 228, 2021, doi: 10.1016/j.ijleo.2020.166201.
[25] J. Kowalewski, T. Mahler, L. Reichardt, et al., "Shape Memory Alloy (SMA)-Based Pattern-Reconfigurable Antenna," IEEE Antennas Wireless Propag. Lett., vol. 12, pp. 1598–1601, 2013, doi: 10.1109/LAWP.2013.2293593.
[26] R. Hussain, M. U. Khan, and M. S. Sharawi, "Design and Analysis of a Miniaturized Meandered Slot-Line-Based Quad-Band Frequency Agile MIMO Antenna," IEEE Transactions on Antennas and Propagation, vol. 68, no. 4, pp. 3005–3014, 2020, doi: 10.1002/jnm.3293.
[27] L. M. Duarte, et al., "Frequency and Pattern Reconfigurable Antenna with Tetra-Circle Fractal Patch Elements," IEEE Antennas Wireless Propag. Lett., vol. 19, no. 10, pp. 1742–1746, 2020, doi: 10.1109/LAWP.2014.2359196.

[28] F. Liu, J. Guo, L. Zhao, et al., "Ceramic Superstrate-Based Decoupling Method for Two Closely Packed Antennas With Cross-Polarization Suppression," IEEE Transactions on Antennas and Propagation, vol. 69, no. 3, pp. 1751–1756, 2020, doi: 10.1109/TAP.2020.3016388.
[29] Y. P. Selvam, et al., "Design of Dual-Band Pattern Reconfigurable Cylindrical Dielectric Resonator Antenna," Int. J. RF Microw. Comput.-Aided Eng., vol. 31, no. 5, 2021, doi: 10.1109/APUSNCURSINRSM.2017.8072926.
[30] J. Zhang, B. Wang, S. Yan, et al., "Metamaterial-Inspired Varactor-Tuned Antenna with Frequency Reconfigurability and Pattern Diversity," Sensors, vol. 24, no. 2, 2024, doi: 10.3390/s24061956.